Indian J Phys
https://doi.org/10.1007/s12648-022-02386-0

ORIGINAL PAPER

Electronic-structural, thermo-electric, and thermo-mechanical properties of M_2AC and M_2AB (M = Nb or Mo, A = Al or Ga) compounds

S Sâad Essaoud[1,2]* and A S Jbara[3]

[1]Department of Physics, Faculty of Science, University of M'sila, 28000, M'sila, Algeria

[2]Laboratoire de Physique des Particules et Physique Statistique, Ecole Normale Supérieure-Kouba, Vieux Kouba, BP 92, 16050 Algiers, Algeria

[3]Mathematics Department, College of Education for Pure Science, Al-Muthanna University, Samawah 66001, Iraq

Received: 11 December 2021 / Accepted: 29 April 2022

Abstract: The effect of constituent atoms on the physical properties of the MAX phase compounds M_2AC and M_2AB (M = Nb or Mo and A = Al or Ga) was studied theoretically. The obtained results showed that each MAX atom affects structural properties such as the equilibrium lattice constants, cohesive energy, and bulk modulus. Also, the thermodynamic stability was confirmed where all compounds have negative formation enthalpies. Voigt–Reuss–Hill approximations have been used to examine the mechanical stability of these compounds; various parameters for this purpose have been found such as Poisson's ratio, shear, bulk modulus, and Young's modulus. We applied the modified Becke–Johnson approximation (mBJ) to calculate the electronic band structure also total and partial density of states. Also, the study expanded towards the thermal properties, where the temperature dependency of the heat capacities at volume (C_v), the entropy (S), and the thermal expansion coefficient (α) are investigated. The semi-local Boltzmann transport theory has been used to investigate thermoelectric properties. By comparing the properties of the compounds according to their constituent atoms, we found that all the studied compounds have ceramic–metallic characters in particular Mo_2AlC alloy, which have high cohesion energy and resist to pressure more than other compounds. In addition, it has electronic conductivity, high thermal conductivity, and a medium thermal absorption coefficient. We also recognized that each compound has a distinguishing feature: Mo_2AlC has isotropic elastic characteristics, although Mo_2GaC has high electrical (σ/τ) and thermal conductivity (κ/τ), whereas Nb_2AlC has a low thermal expansion coefficient, and Nb_2AlB has a greater heat capacity.

Keywords: Thermal conductivity; Thermal expansion; Electrical conductivity; Mechanical properties; Electronic specific heat capacity; Young's modulus; Poisson's ratio

1. Introduction

MAX phase compounds are among materials that have distinctive properties as they combine between ceramic and metallic properties such as high elastic moduli, good high-temperature mechanical properties, good oxidation and corrosion resistance contrary to previously known traditional ceramic properties such as intrinsic brittleness, low thermal expansion coefficient, low fracture toughness and damage tolerance as. On the other hand, they have good thermally and electrically conductivities, deformable at room temperature, readily machinable, thermal shock resistant. All these features found in the MAX phase compounds made them as promising and widely used compounds, as it was found these compounds could be compensated graphite as a material that can withstand high temperatures when heated. This type of compound has got its name for the first time in 2000 by Barsoum [1] where these materials are made up of three types of atoms: transition metal M, atom from A group element, and C or N atom in which all these atoms crystallize in hexagonal structure with $M_{n+1}AX_n$ (n = 1–3) chemical formula.

Recently, many experimental and theoretical studies on this type of materials showed that some of them possess superconductivity character exclusively for ternary carbides M_2AC, where M = Ti, Nb, Mo, and A = S, Ga, As,

*Corresponding author, E-mail: saber.saadessaoud@univ-msila.dz

Published online: 08 June 2022

In, Sn [2]. Also, Bortolozo et al. [3–5] in their work on the compounds Nb_2SnC, Ti_2InC, Nb_2InC, Ti_2InN and Ti_2GeC between the years 2006 and 2012 reveal that these compounds are superconducting at low temperatures. Additionally to many other works concerned with calculating the elastic properties of other materials for this type, among them we mention Bouhemadou et al. have performed a theoretical study on structural and elastic properties on Nb_2InC M_2InC phases and M_2GaC, with M = Ti, V, Nb, and Ta, under pressure effect [6, 7]. Scabarozi et al. [8] were measured the linear thermal expansion coefficient by high-temperature X-ray diffraction and dilatometry of some MAX phase materials. Jonathan et al. [9] have also studied the three compounds Ti_2AlC, Ti_3AlC_2, and Ti_3SiC_2 and calculated their resistivity, in order to use them as surfaces for electrocatalyst support materials in hydrogen fuel cells. Experimentally, Carlos et al. [10] have prepared the MAX phases Ti_2AlC and Ti_3AlC_2 as thin films in high purity via thermal treatment and analyzed them using both XRD and Raman spectroscopy, several properties such as the hardness and the elastic modulus for both MAX phases have been evaluated using nano-indentation tests.

M_2AlB (M = V, Nb, Ta) and M_2AB (M = Ti, Zr, Hf; A = Al, Ga, In) MAX phase borides are studied by Surucu et al. [11, 12]; the findings indicate the dynamic stability for all compounds and the dominant of the ionic bonding through studying electron-density distribution in the (111) plane. On the other hand, a study on the ternary nanolaminated borides M_2AlB_2 (M = Mn, Fe, and Co) [13] reveals that Mn_2AlB_2 is more stable in antiferromagnetic arrangement while the stable magnetic phase of the compounds Fe_2AlB_2 and Co_2AlB_2 is FM. Moreover, among the studied compounds, it has been found that only Co_2AlB_2 is dynamically unstable and that the compound Mn_2AlB_2 has the highest thermal conductivity. Other studies on the same properties have also been performed, including many compounds such as Ti_2SiB by Gencer [14] and M_2SC (M = Ti, Zr, Hf) by He et al. [15]. Other properties that characterize ceramic-metallic materials have been explored and discussed, especially the recent research on the effect of stress on the magnetic properties of Mn_2AlC and Mn_2SiC compounds [16] as well as the study of superconducting phases in a class of metallic ceramics and other properties in many studies carried out by Hadi et al. [17, 18].

In this paper, we present a theoretical study using first-principle density functional calculations on the structural, elastic, electronic, and thermodynamic properties for M_2AC and M_2AB (M = Nb or Mo and A = Al or Ga). By choosing two different atoms for each type of alloy that form the molecule, different important properties of these types of compounds are investigated.

2. Computational methods

Our calculations have been carried out using the full-potential linearized augmented plane wave method (FP-LAPW) implemented in the WIEN2k program [19]. The structural properties have been calculated with both generalized gradient approximation (GGA) [20] and the local density approximation (LSDA) [21] to achieve the exchange–correlation potential, whereas modified Becke–Johnson potential (mBJ) [22] has been used to improve the electronic behavior of all the studied compounds. To study the core and valence electrons separately, the Muffin–Tin approximation is applied where the core electrons are modelled by spherical harmonic functions with angular momentum up to l_{max} = 10 and Gaussian factor G_{max} equal to 12, whereas the valence electrons are depicted by plane wave functions, which are located outside the atomic spheres (interstitial region). The cutoffs of $R_{MT} * K_{max}$ used in our calculation are equal to 8 for all compounds, where K_{max} is the largest reciprocal lattice vector used in the plane wave expansion and R_{MT} represents the smallest MT sphere radii. For Brillouin zone (BZ) integration; a mesh of (17 × 17 × 3) special *k*-points were used for all MAX phase compounds in the irreducible wedge to minimize the total energy for all compounds. The criteria of convergence in the self-consistent were achieved when the difference in energy between two consecutive cycles is less than 10^{-4} Ry. The optimized atomic positions are obtained for minimization of the internal forces to vales less than 10^{-3} Ry/a.u. BoltzTraP [23] and GIBBS2 [24, 25] codes were employed to obtain the thermal and the thermoelectric transport properties, which are based on semi-classical Boltzmann theory and the quasi-harmonic Debye model, respectively. Also, ELASTIC1.1 code [26] is performed to calculate the elastic constants bulk and shear modulus.

3. Results and discussion

3.1. Structural, elastic, electronic, and thermoelectric properties

All the M_2AX compounds studied in this work have a hexagonal structure with space-group (194) P_{63}/mmc. As their structures are shown in Fig. 1(a), we can see that M, A, and X atoms occupy the sites (4*f*) (2*d*) and (2*a*), respectively. So that, the positions atomic of these atoms are given in Table 1. As shown in Fig. 1(b), one "M" atom can stack with three "X" atoms to form a tetrahedron along the *A*-axis.

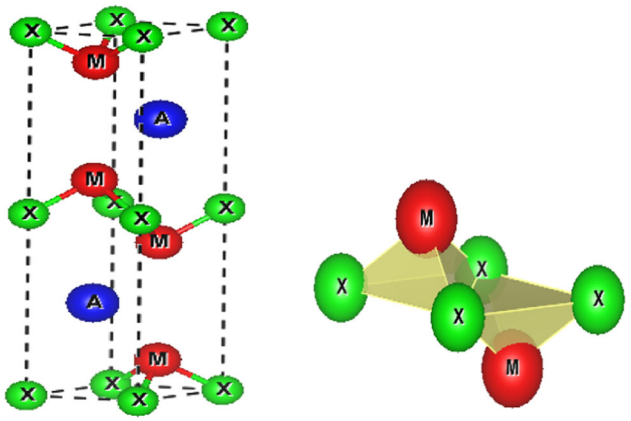

Fig. 1 (**a**) The crystal structure of M_2AX phases (M = Nb or Mo, A = Al or Ga, X = C or B) in hexagonal phase (**b**), linear chain arrangement of MX_3 tetrahedron along the *a*-axis

Before embarking on the calculation of structural properties, we calculated the optimum atomic positions, and this is through using the total energy and force minimization scheme based on Broyden [27, 28]. We have estimated the total energy for various cell volumes and defined the bulk modules for each compound and the equilibrium volume corresponding to the lowest energy, which expresses the most stable state by fitting the *E*–*V* data with Murnaghan equation of state (EOS) [29]. The changing in the *c*/*a* parameter has also been calculated to analyze the structural properties and compared them with the available previous results whether experimental or theoretical values. The results reported in Table 1 reveal that GGA approximation offers rather higher accuracy results for unit cell constants *a* and *c* in consideration of the findings of the other experimental results for all compounds.

Table 1 shows the formation enthalpy computed with the formula (4) and the approximations LDA and GGA. All compounds exhibit negative enthalpies, making them thermodynamically stable and synthesizable [30].

$$\Delta H_{\text{for}}\,(\text{eV/atom}) = \frac{E_{\text{tot}}^{\text{M}_2\text{AX}} - (2E_{\text{solid}}^{\text{M}} + E_{\text{solid}}^{\text{A}} + E_{\text{solid}}^{\text{X}})}{4} \tag{1}$$

$E_{\text{tot}}^{\text{M}_2\text{AX}}$ is the total energy of the unit cell of M_2AX, $E_{\text{solid}}^{\text{M}}$, $E_{\text{solid}}^{\text{A}}$, $E_{\text{solid}}^{\text{X}}$ are the total energies per atom of the solid state of the M, A and X pure elements, respectively.

The bulk modulus and the cohesive energy are among the most important structural properties, where the first term is the resistance of the substance to any external pressure applied to it, while the second term refers to the cohesion and strength of the compound and is represented according to the following formula:

$$E_{\text{coh}}\,(\text{eV/atom}) = \frac{(2E_{\text{atom}}^{\text{M}} + E_{\text{atom}}^{\text{A}} + E_{\text{atom}}^{\text{X}}) - E_{\text{tot}}^{\text{M}_2\text{AX}}}{4} \tag{2}$$

where $N_{\text{M}} + N_{\text{A}} + N_{\text{X}}$ are the sum of the total number of atoms in M_2AX unit-cell, $E_{\text{tot}}^{\text{M}_2\text{AX}}$ the total energy of the

Table 1 Calculated lattice parameters and the formation enthalpies (ΔH_{for}) of M_2AX phases (M = Nb or Mo, A = Al or Ga, X = C or B)

		Nb_2AlC	Nb_2AlB	Nb_2GaC	Nb_2GaB	Mo_2AlC	Mo_2AlB	Mo_2GaC	Mo_2GaB
a (Å)	Z_M	0.0896	0.0907	0.089	0.0916	0.0887	0.0921	0.090	0.091
			0.091[c]	0.089[a]				0.088[a]	
	GGA	3.121	3.194	3.145	3.161	3.031	3.094	3.039	3.076
	LDA	3.083	3.149	3.100	3.112	2.997	3.047	2.996	3.037
	Other *W*	3.115[b]	3.189[b]	3.159[a]		3.029[a]	3.088[a]	3.06[a]	
			3.19[c]						
c (Å)	GGA	13.893	14.025	13.623	14.002	13.464	13.300	13.259	13.271
	LDA	13.720	13.834	13.422	13.781	13.314	13.085	13.060	13.097
	Other *W*	13.939[b]	14.008[b]	13.634[a]		13.448[b]	13.262[b]	13.15[a]	
			13.96[c]						
$\Delta H_{\text{for (eV/atom)}}$	GGA	− 0.65	− 0.54	− 0.75	− 0.68	− 0.33	− 0.44	− 0.38	− 0.51
	LDA	− 0.68	− 0.56	− 0.81	− 0.69	− 0.37	− 0.45	− 0.45	− 0.52
	Other W		− 0.52[c]						

[a]Reference [21]

[b]Reference [31]

[c]Reference [11]

M_2AX unit-cell, and $E^{M}_{atom}, E^{A}_{atom}$ and E^{X}_{atom} the energies of the M, A, and X atoms, respectively.

In order to indicate that the nature of each atom of the M_2AX compound has an effect on both the bulk modulus and the cohesion energy, we have drawn their values as a function of the atoms that form them (see Fig. 2(a) and (b)). This figure reveals that the Mo_2AlC compound has excellent structural properties, high bulk modulus, and high cohesive energy compared to the other compounds. In addition, the results obtained assume that Mo, Al, and C atoms in M, A, and X positions are distinguished by high resistance to deformation and strong cohesive energy compared to Nb, Ga, and B atoms, respectively.

As we have already mentioned, M_2AX compounds have ceramic properties such as hardness, low thermal expansion coefficient and low fracture toughness; therefore, we have examined these characteristics under the influence of the most important factors that ceramic materials may be exposed to pressure resulting from external strain effect on the structure of these compounds. One can see different responses against the applied strain to these materials according to the difference in the internal properties of the structures such as the strength and number of bonds between atoms and the stacking module. The elastic constants are used to calculate the strength and characteristics of the forces in solids. These constants also create a bridge between the mechanical and dynamical characteristics of solids [32]. The elastic constants C_{ij} for all the eight M_2AX compounds using the second-order derivatives of the fitted polynomials of the total energy have been obtained; therefore C_{ij} constants were estimated during the calculation of the total energy as a function of the volume-conserving strains that break the symmetry in the hexagonal structure. Comparing them with each other has also been considered to determine the effect of the nature of the three atoms M, A, and X as well as determining which of them have good properties.

The obtained results such as bulk (B), shear modulus (G), Young's modulus (Y), anisotropy (A), and Poisson's ratio (υ) are listed in Table 2, which calculated as a function of elastic constants C_{ij} using the following formulas [33, 34]:

$$B = \frac{2}{9}\left(C_{11} + C_{12} + 2C_{13} + \frac{C_{33}}{2}\right) \tag{3}$$

$$G = \frac{1}{15}(2C_{11} + C_{33} - C_{12} - 2C_{13}) + \frac{1}{5}\left(2C_{44} + \frac{1}{2}(C_{11} - C_{12})\right) \tag{4}$$

$$Y = \frac{9BG}{3B + G} \tag{5}$$

$$\upsilon = \frac{3B - 2G}{2(3B + G)} \tag{6}$$

$$A = \frac{2C_{44}}{C_{11} - C_{12}} \tag{7}$$

$$f = \frac{C_{11} + C_{12} - 2C_{13}}{C_{33} - C_{13}} \tag{8}$$

According to the elastic properties C_{ij} (Table 2), we can see that all the studied compounds satisfy the mechanical stability criteria of Born Huang ($C_{11} > |C_{12}|, C_{44} > 0$, and $(C_{11} + C_{12})C_{33} > 2C_{13}^2$) [35].

The Bulk modulus (B) of the studied compounds, which expresses the response of these materials against any uniform compression they undergo, was calculated again

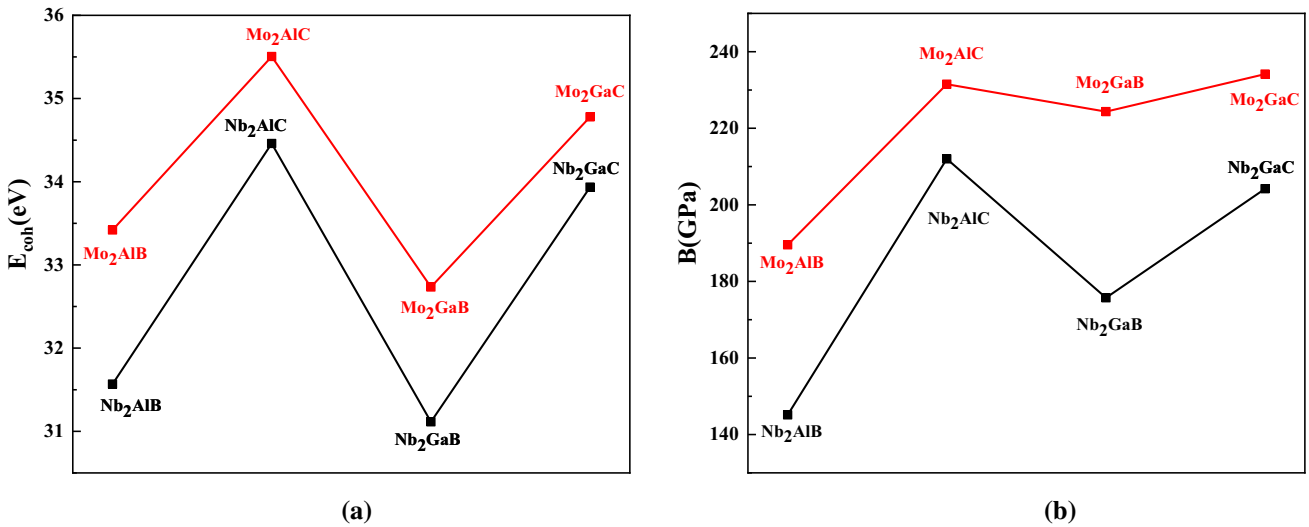

Fig. 2 (**a**) Bulk modulus, and (**b**) cohesive energy of M_2AX phases (M = Nb or Mo, A = Al or Ga, X = C or B) calculated using GGA approximation

Table 2 Elastic constants (C_{ij}), Young's modulus Y, Poisson's ration (υ), Anisotropy (A), Bulk (B) and Shear modulus (G), G/B ratio, f-index, ductility U_d and machinability U_M factors of M_2AX phases (M = Nb or Mo, A = Al or Ga, X = C or B)

	Nb_2AlC	Nb_2AlB	Nb_2GaC	Nb_2GaB	Mo_2AlC	Mo_2AlB	Mo_2GaC	Mo_2GaB
C_{11}	323.5	288.1	345.1	310.3	425.5	318.1	331.4	336.5
	334.0[c]	283.59[b]	374.0[d]		354.4[b]	316.5[b]	306.4[a]	
C_{12}	148.2	113.7	90.7	125.6	65.3	134.7	108.6	89.8
	115.0[c]	91.35[b]	88.0[d]		98.0[b]	105.4[b]	100.6[a]	
C_{13}	141.4	114.6	163.4	120.5	183.6	182.0	220.8	193.9
	149.0[c]	101.69[b]	135.0[d]		146.6[b]	151.7[b]	169.0[a]	
C_{33}	318.3	284.1	316.4	296.4	349.0	240.2	302.8	313.2
	324.0[c]	249.24[b]	310.0[d]		358.9[b]	268.7[b]	302.5[a]	
C_{44}	152.1	143.6	149.6	150.4	180.0	204.6	181.2	192.4
	154.0[c]	125.31[b]	149.0[d]		144.4[b]	161.0[b]	101.8[a]	
B (GPa)	203.02	171.78	204.62	183.35	229.46	208.22	229.56	215.72
	205.0[c]	156.07[b]	196.0[d]		205.05[b]	191.0[b]	250.6[a]	
G (GPa)	114.01	109.36	124.55	115.33	159.19	125.35	122.46	135.53
	119.0[c]	102.42[b]	132.0[d]		127.11[b]	110.8[b]	96.5[a]	
G/B	0.562	0.637	0.609	0.629	0.694	0.602	0.533	0.628
Y	288.09	270.65	310.63	286.02	387.87	313.20	311.91	336.19
	299.0[c]	252.11[b]	323.0[d]		316.04[b]	278.7[b]	256.5[a]	
υ	0.26	0.24	0.25	0.24	0.22	0.25	0.27	0.24
	0.257[c]	0.231[b]	0.249[a]		0.243[b]	0.257[b]	0.329[a]	
A	1.74	1.65	1.18	1.63	1.00	2.23	1.63	1.56
	1.23[b]	1.30[b]			1.12[b]	1.50[b]		
U_d	1.78	1.57	1.64	1.59	1.44	1.66	1.87	1.59
	1.50[b]	1.52[b]			1.61[b]	1.72[b]		
U_M	1.33	1.20	1.37	1.22	1.27	1.02	1.27	1.12
f	1.07	1.02	0.71	1.11	0.75	1.53	− 0.02	0.32
	0.94[b]	1.16[b]			0.75[b]	1.01[b]		

[a]Reference [21]

[b]Reference [31]

[c]Reference [43]

[d]Reference [7]

depending on the elastic constants, and the obtained results are very close to those found in the structural calculations. Also, these results indicated that Mo_2AlC and Mo_2GaC compounds have the greatest ability to resist deformation than other compounds [36]. The shear modulus (G) (shear ability) represents the materials' response to any change in shape [12]. The computed results reveal that Mo_2AlC compounds are malleable compounds with high shear ability compared to the remaining compounds.

Through the three values B, G, and C_{44}, we can estimate the brittleness/ductility and the machinability of the studied materials using ductility $U_d = B/G$ [37] and machinability $U_M = B/C_{44}$ factors [38]. Our results indicate that both Nb_2AlC and Mo_2GaC have a ductile character by calculating Pugh index where this factor expresses the malleability of a material [39], unlike the rest of the compound, where the index was less than 1.75 which they have brittleness character. On the other hand, it becomes obvious that the four compounds Nb_2AlC, Nb_2GaC, Mo_2AlC and Mo_2GaC have higher machinability U_m. The G/B ratio is important for determining a compound's binding type. G/B ratio for dominantly ionic bonding chemicals is approximately 0.6, whereas G/B ratios for dominantly covalent bonding compounds are around 1.1 [36]. According to the findings, G/B ratio values for all of the studied compounds are approximately 0.6, which implied the dominance of the ionic bond.

Young's modulus (Y) is used to measure the stiffness of materials when they obey uniaxial stress averaged over all directions; therefore, we can say based on the calculated values of this parameter that the Mo_2AlC is stiffer than the other compounds. The nature of the bonds formed between atoms in MAX phase compounds whether they are covalent or ionic can be predicted via Poisson's ratio (υ). The

Poisson's ratio values are confined between − 1 and 0.5; usually, it is about 0.1 for typical covalent bonding, 0.25 for typical ionic bonding and 0.33 for typical metallic bonding [40, 41]. Anisotropy of a material (A) determined whether the properties of the crystal are the same in all directions or not when a material undergoes uniform stress. If anisotropy (A) is equal to unity, crystal considers as isotropic, other values greater or smaller than unity its properties change along with different directions. Based on our results, we can see that the anisotropy factors deviate from the unity for most of the studied compounds so these compounds are anisotropic except the Mo_2AlC compounds were which is the only isotropic material. We can also analyze the isotropic character and the strength of the bond along a and c axes by estimating the f-index. According to the value of this indicator, we will evaluate the axis or the plane on which the bonds between the atoms are stronger, since if $f = 1$, then the bonds are equal and isotropic on the axes a and c, while if the value of f is less than 1, the material is stiffer along c axis, while if its value is greater than 1, the bonds on the "ab" plane are stronger than on the c axis. The values of f-index that obtained and reported in the Table 1 appear that Nb_2AlB compound approximately has a similarity in the strength of the bonds along both a and c axes, whereas Nb_2AlC, Nb_2GaB, and Mo_2AlB compounds have strong bonds along the c axis (f larger than 1) in contrary to Nb_2GaC, Mo_2AlC, Mo_2GaC and Mo_2GaB compounds where bonds are stiffer in ab plane than the c-axis (f smaller than 1). We note that the results we obtained about the elastic properties of the studied compounds are very similar to the other results [7, 31, 42, 43].

The electronic behavior of M2AX compounds was studied in this work via computing the band structure as well as the total and partial density of states using the mBJ approximation in treating the exchange–correlation potential. The band structures of M_2AX phases (M = Nb or Mo, A = Al or Ga, X = C or B) at the equilibrium state as calculated using mBJ approximation [22] along high symmetry directions in the first Brillouin zone are plotted in Fig. 3. Through this figure, we can easily observe an overlapping between the conduction and valence bands at the Fermi level, which is proved the metallic behavior of these compounds. To identify the atomic orbits contributing to the formation of both conduction and valence bands, the total and partial density of states (DOS) using mBJ method for M_2AX phase (M = Nb or Mo, A = Al or Ga, X = C or B) have been determined (see Fig. 4). The distribution curve of the contributions of atomic orbitals to the creation of valence and conduction bands indicates that the electrons of the "d" orbitals of Nb and Mo atoms have a higher density of states value at the Fermi level. Therefore, these orbitals have a dominant contribution at the Fermi level, and hence electrons of "d" orbitals have the main role in the conductivity of these materials. As for the contributions of the other atomic orbitals, they were as follows: for M_2AB (M = Nb or Mo, and A = Al or Ga) compounds, the bands in the range (− 9 eV, − 6 eV) arise formed by the strong contribution of the "s" orbit of the "B" atom, while the band extending from − 5 to − 1 eV is formed by the weak contributions of "d" orbitals of M atom, "s" and "p" orbitals of the atom A, "d" of M atom, and the strong contribution of "p" of the atom B. Conduction band extending above the Fermi plane; it is mainly formed by the strong contribution of the "d" orbital of the atom M. For the M_2AC (M = Nb or Mo, and A = Al or Ga) compounds, the contribution of the "s" orbit of the carbon atom shifted to the range between − 11 and − 13 eV and the contribution of the orbital "p" of C atom is greater compared to the case of B atom. As we can refer that obtained results are almost identical to previous studies [17, 31, 42, 44, 45].

Depending on the semi-classical Boltzmann transport theories that implemented in BoltzTraP code [23], the electrical conductivity (σ/τ), thermal conductivity (κ/τ), and electronic specific heat capacity (c) of M_2AC and M_2AB compounds (M = Nb or Mo, A = Al or Ga) at Fermi level for temperature equal to 300 K have been estimated.

The electrical conductivity of material reflects its ability to conduct electric current, with its importance attributed to the mobility of charge carriers (holes and electrons) and carrier concentrations in materials [46]. Figure 5 illustrates the electrical conductivity (σ/τ) coefficient, the electronic thermal conductivity (κ/τ) and electronic specific heat (c) of the free electrons of M_2AC and M_2AB compounds (M = Nb or Mo, A = Al or Ga) in conductivity at ambient temperature 300 K. By observing these curves, we can see similar shapes of curves for the electrical conductivity (σ/τ) coefficient, the electronic thermal conductivity (κ/τ) because both of these parameters are related to each other by the relation of Wiedemann–Franz law $\kappa = L\sigma T$ (L: Lorentz constant) [47]. Therefore, we can assume that Mo_2-based compounds have a higher electrical and thermal conductivity than Nb_2-based compounds, where the maximum values of the two conductivities were found in the two compounds Mo_2GaC and Mo_2AlC. Often, the compounds in which atom X is an atom of "B" has a low thermal and electrical conductivity contrary to in those in which atom X occupies a seed C. The contribution of free electrons in the transfer of heat in solid materials is expressed via the electron heat capacity. According to the values plotted in Fig. 5, it appears that the electron heat capacity has been greater in Mo_2-based compounds, especially when atom B occupies the X position of the M_2AX phase (M = Nb or Mo, A = Al or Ga, X = C or B).

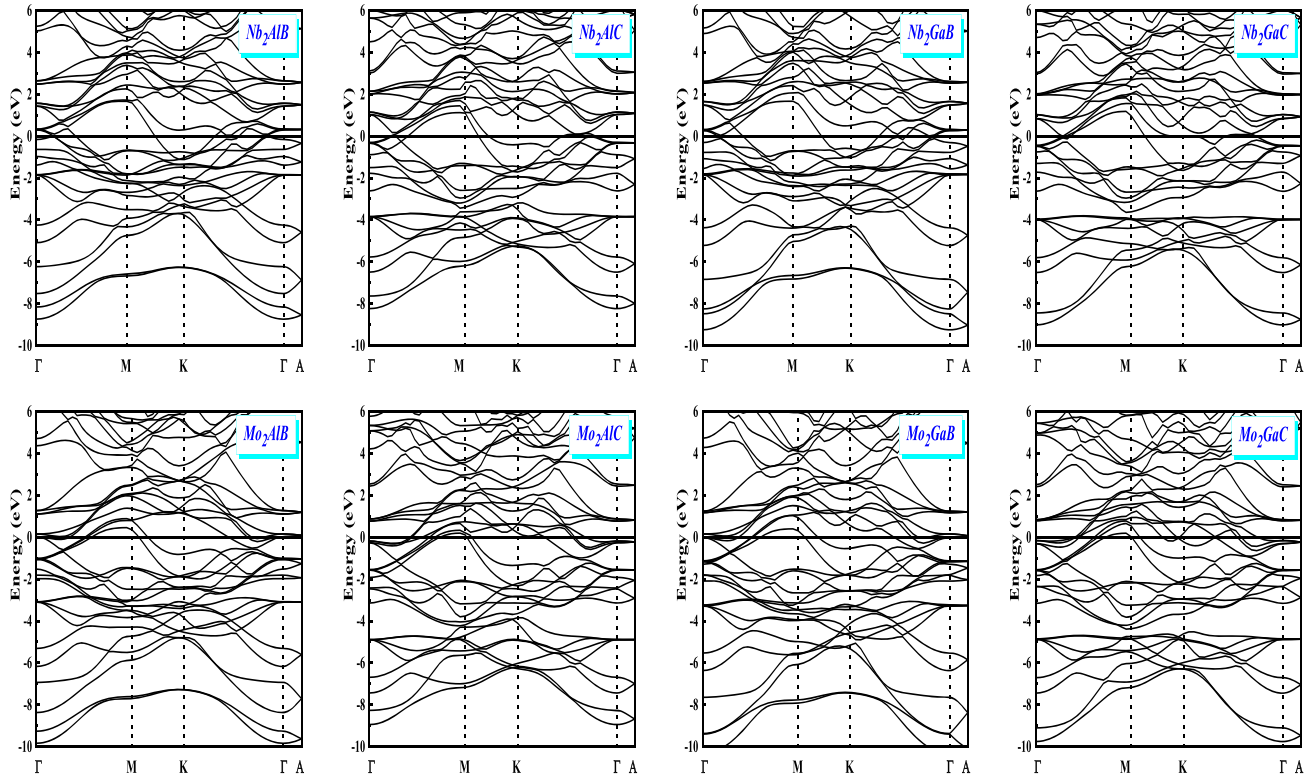

Fig. 3 Band structures of M_2AX phase (M = Nb or Mo, A = Al or Ga, X = C or B) calculated using mBJ approximation

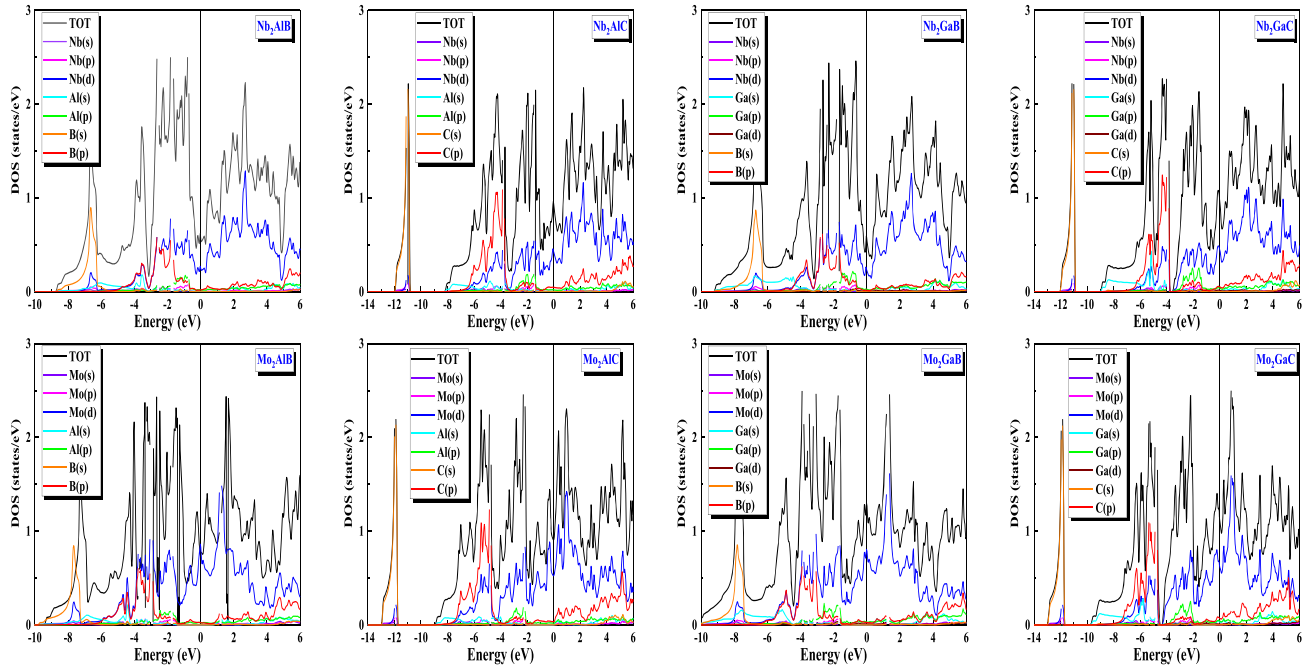

Fig. 4 Total and partial density of states of M_2AX phase (M = Nb or Mo, A = Al or Ga, X = C or B) calculated using mBJ approximation

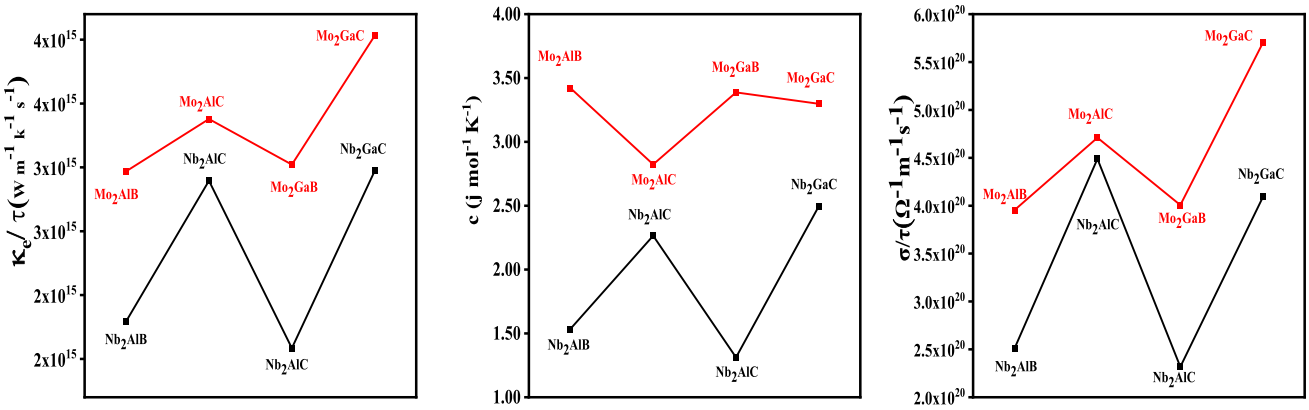

Fig. 5 Electrical conductivity (σ/τ), thermal conductivity (κ/τ) and electronic specific heat capacity (c) of M_2AX phase (M = Nb or Mo, A = Al or Ga, X = C or B) at T = 300 K

3.2. Thermodynamic properties

The first-principle calculation using WIEN2k program is performed at zero temperature, where we neglected the vibrational parts of the atoms in the Hamiltonian equation of the crystal system via applying the Born–Oppenheimer approximation [48]. Here, we have studied the effect of temperature on thermodynamic variables by using the quasi-harmonic model [49] as implemented in GIBBS2 code [24, 25]. The function controlling the phase stability of a solid at a given pressure and temperature is the Gibbs free energy given by:

$$G^*(x,V;P,T) = E_{\text{sta}}(x,V) + PV + A^*_{\text{vib}}(x,V;T) + F^*_{\text{el}}(x,V;T) \tag{9}$$

where E is the total energy, PV corresponds to the hydrostatic condition, A^*_{vib} and F^*_{el} are the non-equilibrium vibrational and electronic free energies, respectively. Debye's model is used to describe the vibrational energy A^*_{vib} in terms of the density of phonon states (the vibrational density of states) $g(\omega)$:

$$A^*_{\text{vib}} = \int_0^{\infty} \left[\frac{\omega}{2} + k_{\text{B}}T\text{Ln}\left(1 - \text{e}^{-\frac{\omega}{k_{\text{B}}T}}\right)\right] g(\omega)\text{d}\omega \tag{10}$$

$$F^*(x,V;T) = E_{\text{sta}}(x,V) + A^*_{\text{vib}}(x,V;T) \tag{11}$$

in this equation, n is the number of atoms per unit volume, D (θ/T) represents the Debye integral, which is given by:

$$D(x) = \frac{3}{x^3}\int_0^{x} \frac{y^3\text{e}^{-y}}{1-\text{e}^{-y}}\text{d}y \tag{12}$$

The equilibrium state (for pressure (P) and a temperature (T) given) is obtained by the minimization of:

$$\left(\frac{\partial G^*(V,P,T)}{\partial V}\right)_{P,T} = 0 \tag{13}$$

Resolving the last equation makes it easy to express the other thermal quantities in particular: entropy (S), the heat capacity at constant volume (C_{v}), and the coefficient of thermal expansion, which are given:

$$S = -3nk_{\text{B}}\ln\left(1-\text{e}^{-\Theta_D/T}\right) + 4nk_{\text{B}}D(\Theta_D/T) \tag{14}$$

$$C_{\text{v}} = 12nk_{\text{B}}D(\Theta_D/T) - \frac{9nk_{\text{B}}\Theta_D/T}{\text{e}^{\Theta_D/T}-1} \tag{15}$$

$$\alpha = -\frac{1}{V}\left(\frac{\partial V}{\partial T}\right)_P = \frac{\gamma\,\text{C}_{\text{v}}}{VB_{\text{T}}} \tag{16}$$

The temperature effect on heat capacities at volume constant (C_{v}), entropy (S) and thermal expansion (α) in the temperature range of 0–1500 K illustrate in Fig. 6. The heat capacity of material represents a substance's ability to absorb energy, and it increases as the number of degrees of freedom for particles increases. On a microscopic scale, entropy can be interpreted as a measure of a system's disorder, and it is considered as a measure of the number of possible configurations. If the temperature increases, the atoms begin to oscillate, allowing new configurations to emerge [46].

Figure 6 demonstrates that the heat capacity at volume constant checked the law of Petit Dulong [50] when the temperature is greater than 700 K and its value set up 100 (J/mol K), while C_{v} is proportional to T^3 at low temperature. At T = 300 K, we can see that Nb_2-based compounds have the highest heat capacities compared to Mo_2-based compounds for the same atoms A and X. Also, the compounds in which an atom B takes the X position have a higher heat absorption capacity C_{v} compared to carbide compounds.

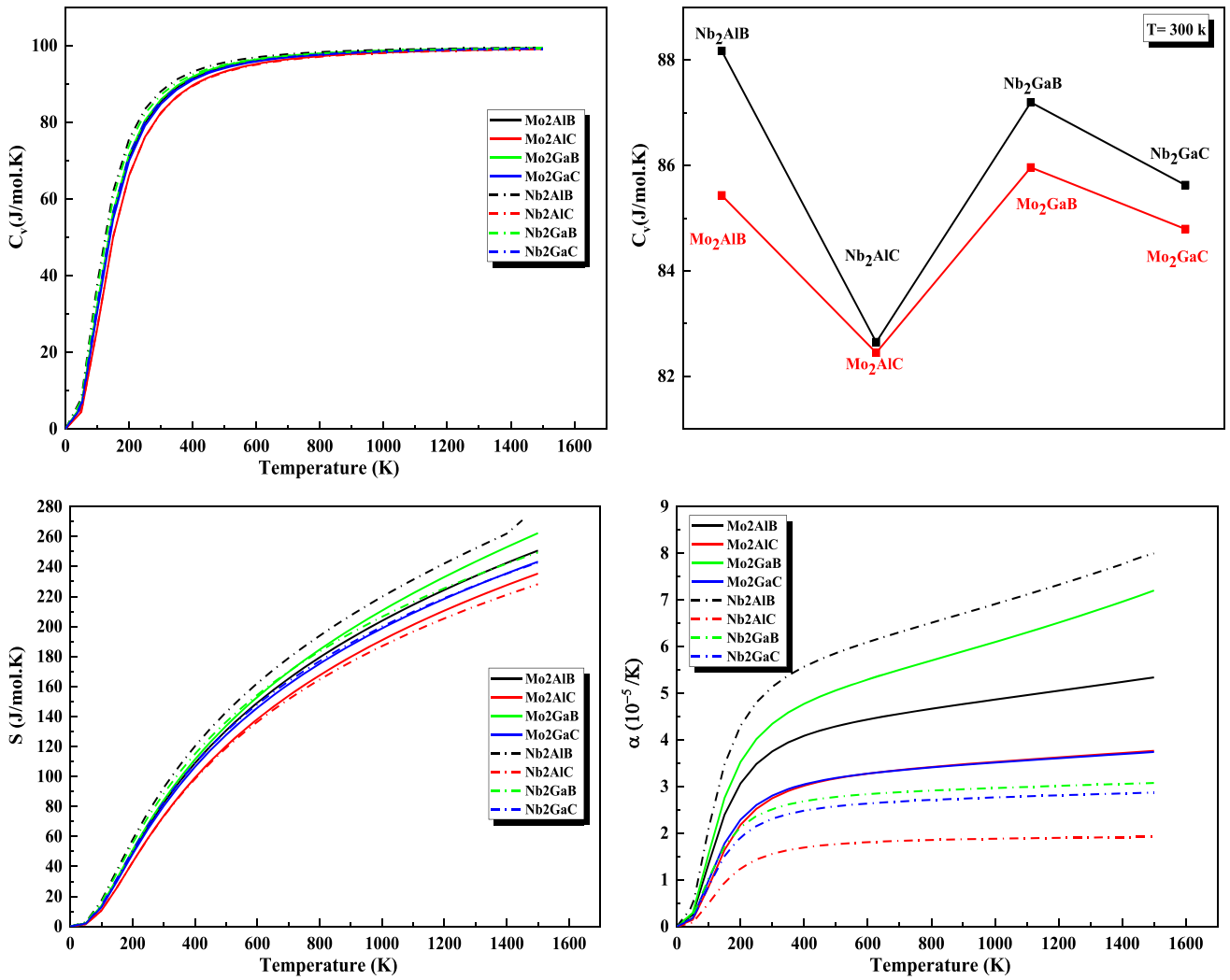

Fig. 6 Temperature dependence of heat capacity (C_V) entropy (S) and coefficient of thermal expansion (α) of M_2AX phase (M = Nb or Mo, A = Al or Ga, X = C or B)

Thermal expansion expresses the proportion of change in unit cell dimension per unit degree temperature change at constant pressure when the temperature changes [51]. For all examined compounds, the thermal expansion coefficient (α) increases very rapidly for temperatures smaller than 200 K, and it increases slowly with temperatures greater than 200 K and becomes almost linear (see Fig. 6). At high-temperature, Nb_2AlC has a low value of thermal expansion coefficient compared to remaining compounds in contrast to the Nb_2AlB, which has great expandability.

Entropy (S) curves that are displayed in Fig. 6 increase with the temperature rising for all M_2AC and M_2AB compounds (M = Nb or Mo, A = Al or Ga) since the increase in the temperature leads to a raise in the number of possible configurations such as the modes of vibration. Noted that all S–T curves of the studied compounds have the same shape where there is no significant difference between the two components studied for the entropy values. Nb_2AlB has the highest entropy value exactly unlike the Nb_2AlC compound, which has the lowest value.

4. Conclusions

Our work included calculating the structural, elastic, electronic, thermal, and thermoelectric properties of M_2AC and M_2AB compounds (M = Nb or Mo, A = Al or Ga) in hexagonal type structure phases using the first principle calculation based on DFT theory. The findings reveal that these compounds had similar properties to ceramic compounds in terms of hardness in addition to the properties of metals, where these properties are affected by the nature of the three-component atoms (M, A, and X). The calculated negative formation enthalpy shows that all M_2AC and M_2AB compounds (M = Nb or Mo, A = Al or Ga) are

thermodynamically stable. Through the calculation of the elastic properties, it was clear to us that all the studied materials are mechanically stable, have great cohesion energy, and have a high resistance coefficient against strain (high bulk modulus), particularly Mo_2AX where the Mo_2AlC is considered as anisotropic material and have lower thermal absorption and medium thermal expansion coefficient. Also, the results have also clarified the dominance of the ionic bond in all compounds. Examining the electronic properties indicates that all these compounds are conductors and have metal behavior, as we find for Mo_2AX materials, which it has greater electrical and thermal conductivity than Nb_2AX materials.

Acknowledgements S. Sâad Essaoud extends his appreciation to the Algerian Ministry of Higher Education and Scientific Research, as well as the General Directorate of Scientific Research and Technological Development, supported this work.

References

[1] M W Barsoum *Prog. Solid State Chem.* **28** 201 (2000)
[2] D Music and J M Schneider *JOM* **59** 60 (2007)
[3] A D Bortolozo et al. *Solid State Commun.* **139** 57 (2006)
[4] A D Bortolozo, O H Sant'Anna, C A M Dos Santos and A J S Machado *Solid State Commun.* **144** 419 (2007)
[5] A D Bortolozo, Z Fisk, O H Sant'Anna, C A M Dos Santos and A J S Machado *Phys. C Supercond.* **469** 256 (2009)
[6] Y Medkour, A Bouhemadou and A Roumili *Solid State Commun.* **148** 459 (2008)
[7] A Bouhemadou and R Khenata *J. Appl. Phys.* **102** 043528 (2007)
[8] T H Scabarozi et al. *J. Appl. Phys.* **105** 013543 (2009)
[9] J Gertzen, P Levecque, T Rampai and T van Heerden *Materials* **14** 77 (2021)
[10] C Torres et al. *Appl. Surf. Sci.* **537** 147864 (2021)
[11] G Surucu, A Gencer, X Wang and O Surucu *J. Alloys Compd.* **819** 153256 (2020)
[12] G Surucu *Mater. Chem. Phys.* **203** 106 (2018)
[13] G Surucu, B Yildiz, A Erkisi, X Wang and O Surucu *J. Alloys Compd.* **838** 155436 (2020)
[14] A Gencer and G Surucu *Mater. Res. Express* **5** 076303 (2018)
[15] X He, Y Bai, Y Li, C Zhu and M Li *Solid State Commun.* **149** 564 (2009)
[16] A Azzouz-Rached, M A Hadi, H Rached, T Hadji, D Rached and A Bouhemadou *J. Alloys Compd.* **885** 160998 (2021)
[17] M A Hadi, N Kelaidis, S H Naqib, A Islam, A Chroneos and R V Vovk *J. Phys. Chem. Solids* **149** 109759 (2021)
[18] M A Hadi *J. Phys. Chem. Solids* **138** 109275 (2020)
[19] P Blaha, K Schwarz, G Madsen, D Kvasnicka and J Luitz (2001)
[20] J P Perdew, K Burke and M Ernzerhof *Phys. Rev. Lett.* **77** 3865 (1996)
[21] W Kohn and L J Sham *Phys. Rev.* **140** A1133 (1965)
[22] A D Becke and E R Johnson *J. Chem. Phys.* **124** 221101 (2006)
[23] G K Madsen and D J Singh *Comput. Phys. Commun.* **175** 67 (2006)
[24] V L A Otero-de-la-Roza and D Abbasi-Pérez *Comput. Phys. Commun.* **182** 2232 (2011)
[25] V L A Otero-de-la-Roza *Comput. Phys. Commun.* **182** 1708 (2011)
[26] R Golesorkhtabar, P Pavone, J Spitaler, P Puschnig and C Draxl *Comput. Phys. Commun.* **184** 1861 (2013)
[27] C G Broyden *IMA J. Appl. Math.* **6** 76 (1970)
[28] C G Broyden *IMA J. Appl. Math.* **6** 222 (1970)
[29] F D Murnaghan *Proc. Natl. Acad. Sci.* **30** 244 (1944)
[30] G Surucu, A Gencer, A Candan, H H Gullu and M Isik *Int. J. Energy Res.* **44** 2345 (2020)
[31] M Khazaei, M Arai, T Sasaki, M Estili and Y Sakka *J. Phys. Condens. Matter* **26** 505503 (2014)
[32] S N Tripathi, V Srivastava, R Khenata and S P Sanyal *Comput. Condens. Matter* **28** e00563 (2021)
[33] M Jamal, S Jalali Asadabadi, I Ahmad and H A Rahnamaye Aliabad *Comput. Mater. Sci.* **95** 592 (2014)
[34] I R Shein and A L Ivanovskii *Phys. Status Solidi B* **248** 228 (2011)
[35] M Born and K Huang *Theory of Crystal Lattices* (Oxford: Clarendon) (1956)
[36] G Surucu, A Candan, A Gencer and M Isik *Int. J. Hydrog. Energy* **44** 30218 (2019)
[37] S F Pugh *Lond. Edinb. Dublin Philos. Mag. J. Sci.* **45** 823 (1954)
[38] M F Cover, O Warschkow, M M M Bilek and D R McKenzie *J. Phys. Condens. Matter* **21** 305403 (2009)
[39] A Benamer, Y Medkour, S S Essaoud, S Chaddadi and A Roumili *Solid State Commun.* **331** 114305 (2021)
[40] S N Tripathi, V Srivastava and S P Sanyal *J. Supercond. Nov. Magn.* **32** 2931 (2019)
[41] S N Tripathi, V Srivastava, H Pawar and S P Sanyal *Indian J. Phys.* **94** 1195 (2020)
[42] I R Shein and A L Ivanovskii *Phys. C Supercond.* **470** 533 (2010)
[43] Z Sun, S Li, R Ahuja and J M Schneider *Solid State Commun.* **129** 589 (2004)
[44] J Wang and Y Zhou *Phys. Rev. B* **69** 214111 (2004)
[45] M A Hadi, M S Ali, S H Naqib and A Islam *Int. J. Comput. Mater. Sci. Eng.* **2** 1350007 (2013)
[46] S S Essaoud and A S Jbara *J. Magn. Magn. Mater.* 167984 (2021)
[47] G V Chester and A Thellung *Proc. Phys. Soc. 1958–1967* **77** 1005 (1961)
[48] M Born and R Oppenheimer *Ann. Phys.* **389** 457 (1927)
[49] P Debye *Ann. Phys.* **386** 1154 (1926)
[50] P L Dulong and A-T Petit *Recherches sur quelques points importans de la theorie de la Chaleur* (1819)
[51] M E Ketfi, H Bennacer, S S Essaoud, M I Ziane and A Boukortt *Mater. Chem. Phys.* 125553 (2021)